Modulation of the Local SR Ca^{2+} Release by Intracellular Mg^{2+} in Cardiac Myocytes

Konstantin Gusev and Ernst Niggli

Department of Physiology, University of Bern, 3012 Bern, Switzerland

In cardiac muscle, Ca^{2+}-induced Ca^{2+} release (CICR) from the sarcoplasmic reticulum (SR) defines the amplitude and time course of the Ca^{2+} transient. The global elevation of the intracellular Ca^{2+} concentration arises from the spatial and temporal summation of elementary Ca^{2+} release events, Ca^{2+} sparks. Ca^{2+} sparks represent the concerted opening of a group of ryanodine receptors (RYRs), which are under the control of several modulatory proteins and diffusible cytoplasmic factors (e.g., Ca^{2+}, Mg^{2+}, and ATP). Here, we examined by which mechanism the free intracellular Mg^{2+} ($[Mg^{2+}]_{free}$) affects various Ca^{2+} spark parameters in permeabilized mouse ventricular myocytes, such as spark frequency, duration, rise time, and full width, at half magnitude and half maximal duration. Varying the levels of free ATP and Mg^{2+} in specifically designed solutions allowed us to separate the inhibition of RYRs by Mg^{2+} from the possible activation by ATP and Mg^{2+}-ATP via the adenine binding site of the channel. Changes in $[Mg^{2+}]_{free}$ generally led to biphasic alterations of the Ca^{2+} spark frequency. For example, lowering $[Mg^{2+}]_{free}$ resulted in an abrupt increase of spark frequency, which slowly recovered toward the initial level, presumably as a result of SR Ca^{2+} depletion. Fitting the Ca^{2+} spark inhibition by $[Mg^{2+}]_{free}$ with a Hill equation revealed a K_i of 0.1 mM. In conclusion, our results support the notion that local Ca^{2+} release and Ca^{2+} sparks are modulated by Mg^{2+} in the intracellular environment. This seems to occur predominantly by hindering Ca^{2+}-dependent activation of the RYRs through competitive Mg^{2+} occupancy of the high-affinity activation site of the channels. These findings help to characterize CICR in cardiac muscle under normal and pathological conditions, where the levels of Mg^{2+} and ATP can change.

INTRODUCTION

Control of intracellular Ca^{2+} homeostasis plays a central role in excitation-contraction coupling of cardiac myocytes. The action potential and depolarization of the cell membrane leads to activation of L-type Ca^{2+} channels. The resulting influx of Ca^{2+} initiates CICR from the SR. This Ca^{2+} release occurs through Ca^{2+} channels of the SR, called RYRs, which are of the type II isoform (RYR2) in cardiac myocytes (Otsu et al., 1990). The global cytosolic elevation of the intracellular Ca^{2+} concentration ($[Ca^{2+}]_i$) arises from the spatial and temporal summation of elementary Ca^{2+} release events, Ca^{2+} sparks (Cheng et al., 1993; Niggli and Shirokova, 2007). It appears that these local Ca^{2+} release events represent the concerted opening of a group of RYR2 (Niggli, 1999; Wang et al., 2001; Berridge, 2006). To reestablish the resting intracellular Ca^{2+} concentration, Ca^{2+} ions are sequestered back into SR by the Ca^{2+} pump (SERCA) while Ca^{2+} entering via L-type Ca^{2+} current is extruded from the cell via the Na^{+}-Ca^{2+} exchanger.

The SR Ca^{2+} release process itself is regulated both by cytosolic Ca^{2+} and by Ca^{2+} from the luminal side of SR, which appears to modulate the cytosolic Ca^{2+} sensitivity (DelPrincipe et al., 1999; Meissner, 2002; Laver, 2005; Keller et al., 2007; Gyorke and Terentyev, 2008). Besides a variety of regulatory proteins located in the RYR macromolecular complex, several diffusible modulators of the RYR have been described, most notably Mg^{2+} and ATP (Fabiato and Fabiato, 1975; Meissner, 2002), the concentrations of which are interdependent because of Mg^{2+} buffering by ATP. At rest, cardiac myocytes contain around 3–5 mM of total ATP and 0.5–1.2 mM of free Mg^{2+} (Hess et al., 1982; Blatter and McGuigan, 1986). In ischemia the concentration of ATP declines, whereas the concentration of free Mg^{2+} ($[Mg^{2+}]_{free}$) is known to rise around threefold (Murphy et al., 1989; Kléber, 1990).

Mg^{2+} ions have been shown to suppress SR calcium release in a variety of skeletal and cardiac muscle preparations. It is suggested that Mg^{2+} interacts with Ca^{2+}-activating and -inactivating sites on the RYRs, the A-site and I-site, respectively (Laver et al., 1997a). As $[Mg^{2+}]_{free}$ is lowered, Mg^{2+} dissociates from the low-affinity I-site at which binding of either Ca^{2+} or Mg^{2+} inhibits channel opening. At even lower $[Mg^{2+}]_{free}$, it also dissociates from the high-affinity A-site at which either Ca^{2+} or Mg^{2+} can bind, but at which only Ca^{2+} activates the channel, whereas Mg^{2+} binding at this site competitively inhibits

Correspondence to Ernst Niggli: niggli@pyl.unibe.ch

The online version of this article contains supplemental material.

The Rockefeller University Press $30.00
J. Gen. Physiol. Vol. 132 No. 6 721–730
www.jgp.org/cgi/doi/10.1085/jgp.200810119

Ca^{2+} activation (Ashley and Williams, 1990; Laver et al., 1997b).

Very recently, Mg^{2+} has been suggested to also exhibit a stimulating effect on RYR2 in an intermediate concentration range of Ca^{2+} (10–100 µM) (Chugun et al., 2007). These authors showed that Mg^{2+} renders the RYR2 more sensitive to modulators of CICR, such as caffeine, β,γ-methylene ATP, procaine, and calmodulin. These new findings suggest that the role of Mg^{2+} may be more complex than previously thought.

Most experiments characterizing the interactions of Mg^{2+} with the RYRs were conducted using lipid bilayers, SR vesicles, or skinned muscle fibers (Lamb, 2000; Meissner, 2004). These studies have yielded important information about the interactions between Mg^{2+} and RYRs on the molecular level. However, much less data are available describing how these observations are applicable to CICR and the generation of Ca^{2+} sparks in cardiac myocytes, under more physiological conditions and with preserved ultrastructure. Although an inhibition of Ca^{2+} spark formation by elevated Mg^{2+} concentrations has been reported in permeabilized cardiomyocytes (Lukyanenko et al., 2001), the phenomenon was not studied in detail and virtually no information is available for low Mg^{2+} concentrations. Some studies have been published describing the behavior of RYRs and Ca^{2+} sparks at different $[Mg^{2+}]$ in frog skeletal muscle (Lacampagne et al., 1998; Shtifman et al., 2002; Zhou et al., 2004), but these findings may be quite different from those one would expect in cardiomyocytes. There are numerous differences between the skeletal and cardiac RYR isoforms, such as, for example, activation and inactivation by Ca^{2+}, ATP, and caffeine (Lamb, 2000; Copello et al., 2002). Finally, the Mg^{2+} modulation of RYR2 is important not only for understanding its role in Ca^{2+} homeostasis and fluxes, but also for interpreting changes of Ca^{2+} signaling under ischemic conditions, where $[Mg^{2+}]_i$ is elevated (and [ATP] is low).

Here, we analyzed spatiotemporal features of Ca^{2+} sparks recorded from permeabilized mouse ventricular myocytes at different intracellular concentrations of Mg^{2+} and ATP. The findings indirectly reflect the activity of the RYRs in their natural microenvironment as a function of $[Mg^{2+}]_{free}$ and $[ATP]_{free}$ and allowed us to identify the predominant mechanism for Ca^{2+} spark modulation by Mg^{2+} and ATP in cardiac myocytes.

MATERIALS AND METHODS

Isolation of Cardiomyocytes

Animals were housed and handled according to the guidelines of the Swiss Animal Protection law, and the experiments were conducted in accordance with the Guide for the Care and Use of Laboratory Animals (1996, National Academy of Sciences, Washington, DC). Cardiac ventricular myocytes were isolated from adult mice using established enzymatic procedures as described previously (Szentesi et al., 2004). In brief, mice were killed by cervical dislocation and the excised hearts were mounted on a Langendorff perfusion system. After perfusion with nominally Ca^{2+}-free Tyrode's solution for 3–5 min, 14 U/ml collagenase II (Worthington type 2), 0.2 U/ml protease (type XIV; Sigma-Aldrich), and 50 µM Ca^{2+} were added to the solution. After an additional 6–9 min of perfusion, the hearts were removed from the Langendorff apparatus and cut in small pieces, followed by gentle trituration to obtain a cell suspension. Subsequently, the Ca^{2+} concentration was slowly raised to the final concentration of 1.8 mM.

Cell Permeabilization and Confocal Ca^{2+} Imaging

Isolated cardiac myocytes were permeabilized by exposure to saponin (0.005%; 30–45 s) in recording solution that contained: 110 mM K^+ aspartate, 1 mM EGTA, 10 mM phosphocreatine, 5 U/ml creatine phosphokinase, 5 mM reduced L-glutathione, 4% dextran (mol wt 40,000), 50 µM fluo-3, and 10 mM HEPES, pH 7.2. Concentration of $[Ca^{2+}]_{free}$ was adjusted to 50 nM, and concentrations of Mg^{2+} and ATP of the various solutions are shown in Table I. $[Ca^{2+}]_{free}$, $[Mg^{2+}]_{free}$, and $[ATP]_{free}$ concentrations were calculated using WebMAX 10/06 software (http://www.stanford.edu/~cpatton/maxc.html). In addition, $[Ca^{2+}]_{free}$ was confirmed to be within ±4 nM of the calculated values using a fluorescence spectrometer (NanoDrop 3300; NanoDrop Products) and the ratiometric indicators Indo-1. Averaged measurements for $[Mg^{2+}]_{free}$ with Mag-Indo-1 were exactly as calculated. The free Ca^{2+} concentration of 50 nM is very close to the recently measured 42 nM in resting mouse cardiomyocytes (Williams and Allen, 2007) and was chosen to have a nonzero resting spark frequency. During all experiments, the solutions were exchanged by complete replacement. Fluo-3 was excited with the 488-nm line of an argon-ion laser. Fluorescence was detected at >500 nm with a confocal laser-scanning microscope operating in line-scan mode (500 lines/s; *µRadiance* [Bio-Rad Laboratories]; 60× water-immersion objective [DIC H; Nikon]). The fluorescence was normalized and expressed as F/F_0, where F_0 is the baseline fluorescence at the beginning of each recording. The frequency and spatiotemporal parameters of the Ca^{2+} sparks were determined from the line-scan images using a computer algorithm similar to that described previously (Cheng et al., 1999; Rios et al., 2001). Ca^{2+} spark frequencies were expressed as the number of recorded sparks per

TABLE I

Calculated Concentrations of $[Mg^{2+}]_{free}$, Free [ATP], and [MgATP] in Solutions Used in Different Sets of Experiments

	Mg^{2+}_{total}	Mg^{2+}_{free}	ATP_{total}	ATP_{free}	Mg-ATP
A	0.00	**0.00**	3.00	**3.00**	0.00
	1.53	**0.10**	3.00	**1.58**	1.42
	2.14	**0.20**	3.00	**1.07**	1.93
	2.97	**0.50**	3.00	**0.54**	2.46
	3.73	**1.00**	3.00	**0.30**	2.70
	5.99	**3.00**	3.00	**0.11**	2.89
B	0.39	0.20	0.29	**0.10**	0.19
	2.14	0.20	3.00	**1.07**	1.93
	5.61	0.20	8.40	**3.00**	5.40
C	0.00	**0.00**	0.30	0.30	0.00
	0.37	**0.10**	0.57	0.30	0.27
	0.75	**0.20**	0.84	0.30	0.54
	1.87	**0.50**	1.65	0.30	1.35
	3.73	**1.00**	3.00	0.30	2.70
	11.20	**3.00**	8.40	0.30	8.10

(A) In this set of solutions, total ATP remains constant, but $[Mg^{2+}]_{free}$ and $[ATP]_{free}$ both vary. (B) $[Mg^{2+}]_{free}$ is kept constant. (C) $[Mg^{2+}]_{free}$ is variable but $[ATP]_{free}$ is constant. Values representing variable $[Mg^{2+}]_{free}$ or $[ATP]_{free}$ are shown in bold for clarity.

second and per 100 µm of scanned distance. All experiments were performed at room temperature (20–22°C).

Data Analysis

Data from line-scan images were averaged during the indicated intervals within each cell and are presented as mean ± SEM obtained from *n* different cells. Statistical differences between datasets were evaluated by Student's *t* test. Significance (*) was defined at $P < 0.05$. For multivariate analysis of Ca^{2+} sparks, we applied a random-effects linear regression model using the inverse of the variance of the Ca^{2+} spark frequency as analytical weight, mean spark frequency as dependent variable, and $[Mg^{2+}]$, [ATP], and [MgATP] as independent variables. Statistical analyses were performed in Stata software (version 10; Stata Corp.).

Online Supplemental Material

Video 1 contains the animation of a surface plot showing Ca^{2+} spark frequency as a function of both $[Mg^{2+}]_{free}$ and $[ATP]_{free}$. In addition, Table S1 lists detailed results of the univariable and bivariable regression analysis. The online supplemental material is available at http://www.jgp.org/cgi/content/full/jgp.200810119/DC1.

RESULTS

Free $[Mg^{2+}]$ Affects Local Ca^{2+} Sparks

In a first series of experiments, we examined how different free Mg^{2+} concentrations affected the local Ca^{2+} release events (Ca^{2+} sparks) at a constant level of total ATP ($[ATP]_{total}$ = 3 mM; for solution composition see Table I, A). Cardiomyocytes were permeabilized and initially bathed in control solution containing 1 mM $[Mg^{2+}]_{free}$. After acquiring confocal line-scan images during ~4 min in control, the solution was rapidly exchanged with various test concentrations of free Mg^{2+} (in the range of 0–3 mM). As already evident from the raw confocal line-scan images taken immediately after the solution change and 4 min later, this generally lead to biphasic changes in the Ca^{2+} spark frequency (Fig. 1). When analyzing the time-course of the spark frequency, we noted transient changes within the first few seconds, after which the spark frequency approached a new steady-state (Fig. 2 A). For example, lowering $[Mg^{2+}]_{free}$ resulted in an abrupt and up to fourfold increase in spark frequency, which subsequently declined almost to the control level. In contrast, increasing $[Mg^{2+}]_{free}$ induced a reduction of the spark frequency, which then partly recovered to an intermediate level. The maximal frequency was maintained only transiently and was limited to the first few seconds after solution exchange, as it can be clearly seen in the trace with nominally 0 mM $[Mg^{2+}]_{free}$. Therefore, for further analysis we divided the data into two groups:

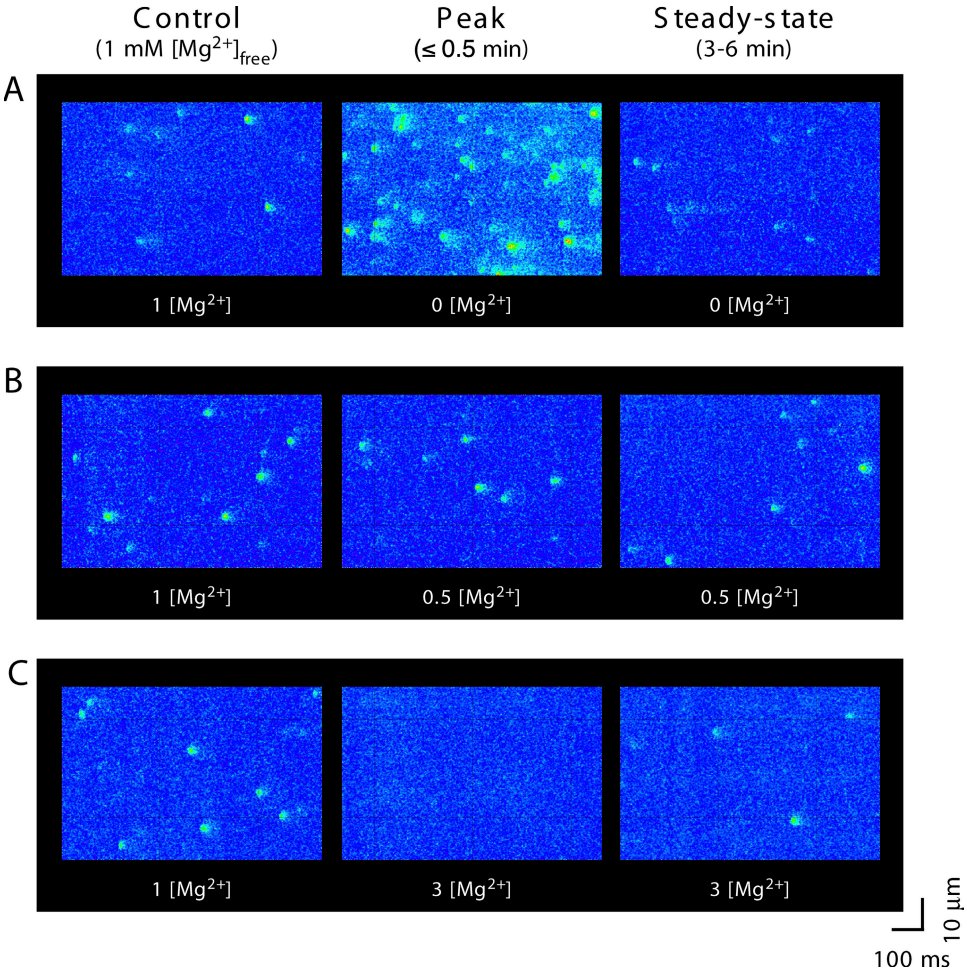

Figure 1. Changes in $[Mg^{2+}]_{free}$ affect the frequency of spontaneous Ca^{2+} sparks. Representative examples of confocal line-scan images recorded from permeabilized cardiomyocytes. (A) Solution change from 1 mM $[Mg^{2+}]_{free}$ (control) to nominally Mg^{2+} free (with 3 mM $[ATP]_{free}$). (B) To 0.5 mM $[Mg^{2+}]$ (with 0.54 mM $[ATP]_{free}$). (C) To 3 mM $[Mg^{2+}]$ (with 0.11 mM $[ATP]_{free}$). The images were obtained before the solution change (left; 1 mM $[Mg^{2+}]$), 5–30 s after (middle), and 3–6 min after (right) exchange of solution.

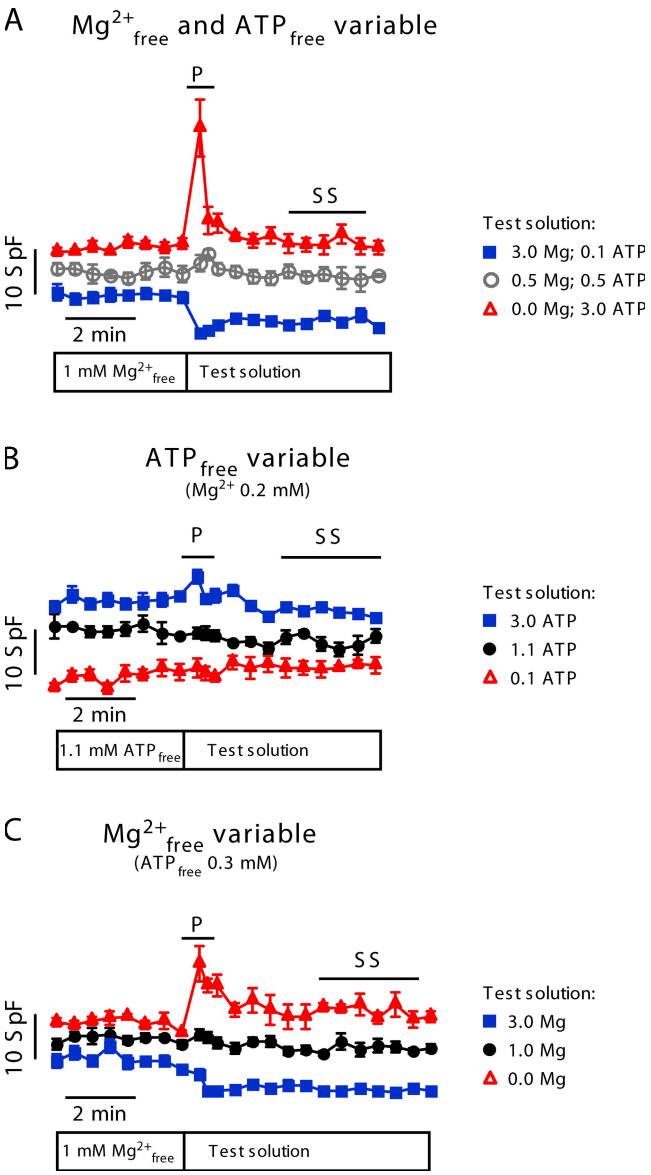

Figure 2. Time-course of averaged Ca^{2+} spark frequencies after changes in $[Mg^{2+}]_{free}$ and $[ATP]_{free}$. Traces are offset slightly for clarity. SpF denotes spark frequency (per s^{-1} 100 μm^{-1}). $[Mg^{2+}]_{free}$ was initially 1 mM in all experiments (control solution). For composition of the test solution, see symbol legend on the right. (A) At the moment indicated by the bar below the traces, test solutions were applied with different levels of $[Mg^{2+}]_{free}$ and $[ATP]_{free}$, but at constant ATP_{total} (3 mM). (B) $[ATP]_{free}$ was varied at constant $[Mg^{2+}]_{free}$ (0.2 mM). (C) $[Mg^{2+}]_{free}$ was varied at constant $[ATP]_{free}$ (0.3 mM). Time intervals for data considered in further analyses are indicated by horizontal lines. P, peak values; SS, steady-state values.

(1) the peak changes (1–15 s after the solution switch), and (2) the steady-state measurements (3–6 min after solution exchange). The data are summarized in Fig. 3 A, where peak values are shown in gray and steady-state frequency in black. As noticeable when comparing the gray with the black trace in Fig. 3 A (left), the spark steady-state frequency recovered more completely upon reducing $[Mg^{2+}]_{free}$ than upon increasing $[Mg^{2+}]_{free}$ to 3 mM.

As a complication for the interpretation of these observations, the open probability of the RYRs also depends on ATP because the channel has an activating adenine binding site (Kermode et al., 1998). Taking this complexity into account, the changes in Ca^{2+} spark frequency as a function of $[Mg^{2+}]_{free}$ observed in our experiments could also be attributed to variations in $[ATP]_{free}$ (or [MgATP]) because the concentrations of the three compounds are interdependent. Therefore, we re-plotted our results in dependence of $[ATP]_{free}$ and [MgATP] (Fig. 3; see also Fig. 4). Indeed, the high frequency of Ca^{2+} sparks also correlated with a high concentration of $[ATP]_{free}$, which corresponds to the solution with low $[Mg^{2+}]_{free}$ (Fig. 3 A, middle). Thus, our observations could, in principle, also be explained by the activation of the RYRs by $[ATP]_{free}$. However, the dependence of the spark frequency on [MgATP] was the opposite of what one would expect for RYR activation by [MgATP], and therefore we could rule out [MgATP] as a main activator of Ca^{2+} sparks (Fig. 3 A, right).

Because Ca^{2+} sparks represent a major pathway for the SR Ca^{2+} leak, some of the observations were transient because of secondary alterations of SR Ca^{2+} content subsequent to increases (or decreases) of the spark frequency. This is because Ca^{2+} spark frequency and some of the spatiotemporal spark parameters also strongly depend on the SR Ca^{2+} loading, as RYRs are regulated by luminal Ca^{2+} (Lukyanenko et al., 2001; Laver, 2005; Keller et al., 2007). To estimate these changes in SR Ca^{2+} content, we rapidly applied a solution containing 20 mM caffeine at the end of the experiment (Fig. 5 A). We noted that increasing $[Mg^{2+}]_{free}$ to 3 mM lead to an accumulation of Ca^{2+} inside the SR, whereas a reduction of $[Mg^{2+}]_{free}$ resulted in a lower SR Ca^{2+} content, as expected.

Free [ATP] Only Slightly Affects Spark Frequency

We next investigated whether binding of ATP to the adenine binding site of the RYR could be the mechanism responsible for our observations (Kermode et al., 1998; Yang and Steele, 2001; Meissner, 2004). The EC_{50} for channel activation by ATP has been estimated to be 0.2 mM for sheep cardiac RYR (Kermode et al., 1998). This is in the range of concentrations present in our experiments (0.11–3 mM; Table I, A). Therefore, we decided to examine the Ca^{2+} spark properties in the range of 0.1–3 mM $[ATP]_{free}$ with solutions designed to have a constant concentration of $[Mg^{2+}]_{free}$ (0.2 mM; see Table I, B). As shown in Fig. 2 B, in these experiments the observed changes in Ca^{2+} spark frequency were quite small. Only the highest level of $[ATP]_{free}$ resulted in a modest transient increase, which may correlate with an activation of the RYRs by ATP (Figs. 2 B and 3 B). Collectively, varying $[ATP]_{free}$ at constant $[Mg^{2+}]_{free}$ affected sparks properties much less than when changing $[Mg^{2+}]_{free}$ (compare Fig. 3, A and B).

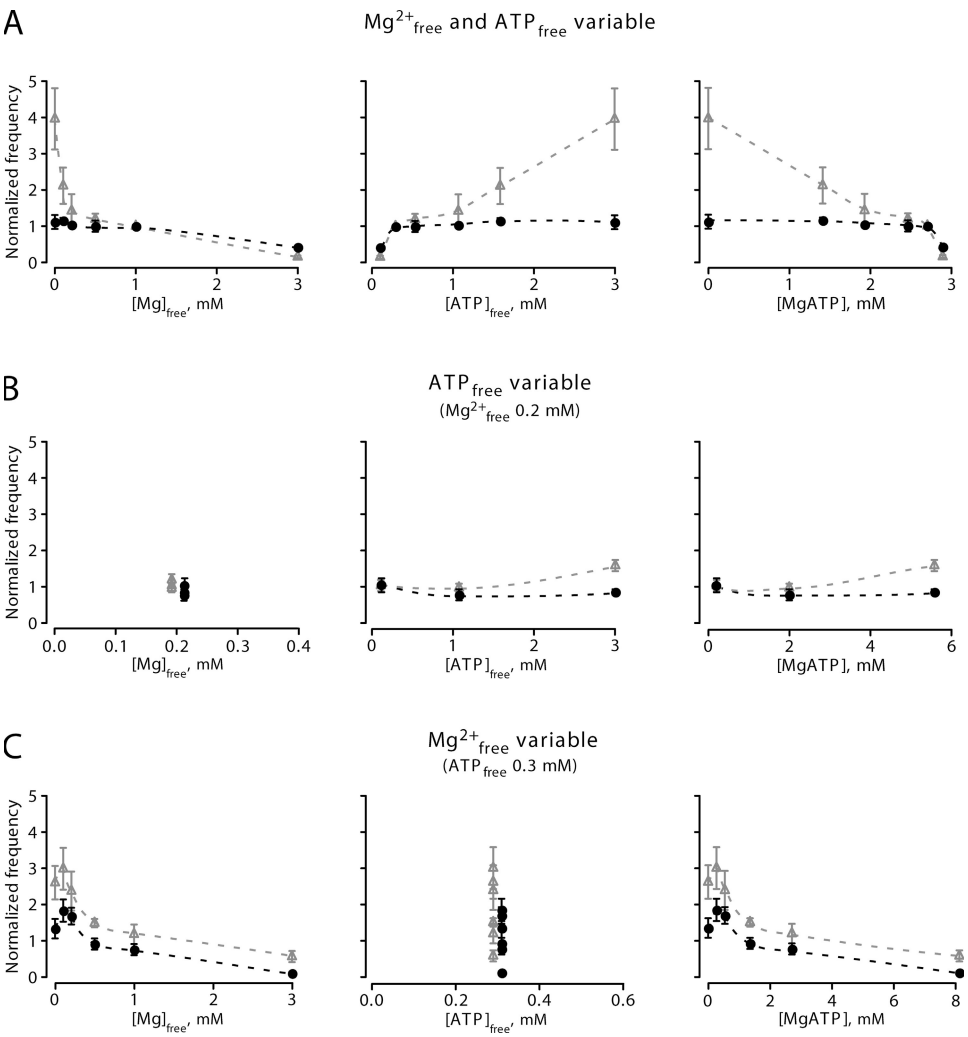

Figure 3. Summary of Ca^{2+} spark frequency variations and their dependence on $[Mg^{2+}]_{free}$, $[ATP]_{free}$, and [MgATP]. Spark frequencies were determined from the peak (P; 0–30 s; gray triangles and lines) and from the steady-state (SS; 3–6 min; black circles and lines) after solution exchange, as shown by lines in Fig. 2. (A) Spark frequencies at constant total ATP ($[Mg^{2+}]_{free}$ and $[ATP]_{free}$ varied simultaneously). (B) Spark frequencies at constant $[Mg^{2+}]_{free}$ (0.2 mM) but variable $[ATP]_{free}$. (C) Spark frequencies at constant $[ATP]_{free}$ (0.3 mM) but variable $[Mg^{2+}]_{free}$. The spark frequencies were plotted versus $[Mg^{2+}]_{free}$ (left), $[ATP]_{free}$ (middle), and [MgATP] (right) to isolate the dependence on each compound from the others.

To reveal differences in the SR Ca^{2+} load as a function of $[ATP]_{free}$, we applied 20 mM caffeine at the end of each experiment. Again, the findings were opposite to the results observed before; lowering $[ATP]_{free}$ to 0.1 mM resulted in a reduction of the SR Ca^{2+} load (Fig. 5 B). However, increasing $[ATP]_{free}$ from 1.1 to 3 mM did not change SR Ca^{2+} loading much.

Changing $[Mg^{2+}]_{free}$ at Constant $[ATP]_{free}$ Affects Ca^{2+} Sparks

Another approach to avoid a possible interference by free [ATP] and to isolate the Ca^{2+} spark modulation by Mg^{2+} is to design solutions in which $[ATP]_{free}$ remains constant despite changes of $[Mg^{2+}]_{free}$. Thus, we next performed a series of experiments at constant $[ATP]_{free}$ (0.3 mM) while varying the $[Mg^{2+}]_{free}$ from 0 to 3 mM (solutions in Table I, C). Again, we observed transient changes of the Ca^{2+} spark frequency immediately after the change of solution (Fig. 2 C). However, in this series of experiments, the adjustments of the steady-state levels were somewhat more pronounced than in the initial experiments (Fig. 3 C). As before, the steady-state SR Ca^{2+} content was dependent on $[Mg^{2+}]_{free}$ (Fig. 5 C). Note that even after 4–6 min in nominally Mg^{2+}-free solution, Ca^{2+} sparks were still detectable and the store not yet completely empty.

Multivariate Statistical Analysis of Ca^{2+} Spark Frequencies

As already mentioned, in our experiments the Ca^{2+} spark frequency depended on several variables that are interdependent (e.g., $[Mg^{2+}]_{free}$, $[ATP]_{free}$, [MgATP], and SR Ca^{2+} content). This complication was the main reason to design several sets of solutions that simplify this problem by keeping at least one variable constant. An alternative approach is to analyze the dataset with multivariate statistical methods. We applied a random-effects linear regression model to determine these more complex relationships. To simplify the analysis somewhat, we made the following assumption: we assumed that immediately after the solution change the Ca^{2+} concentration inside the SR has not yet changed. Collectively, the bivariable analysis essentially revealed the same correlations and dependencies we had derived from the specifically designed solutions: a significant negative association between

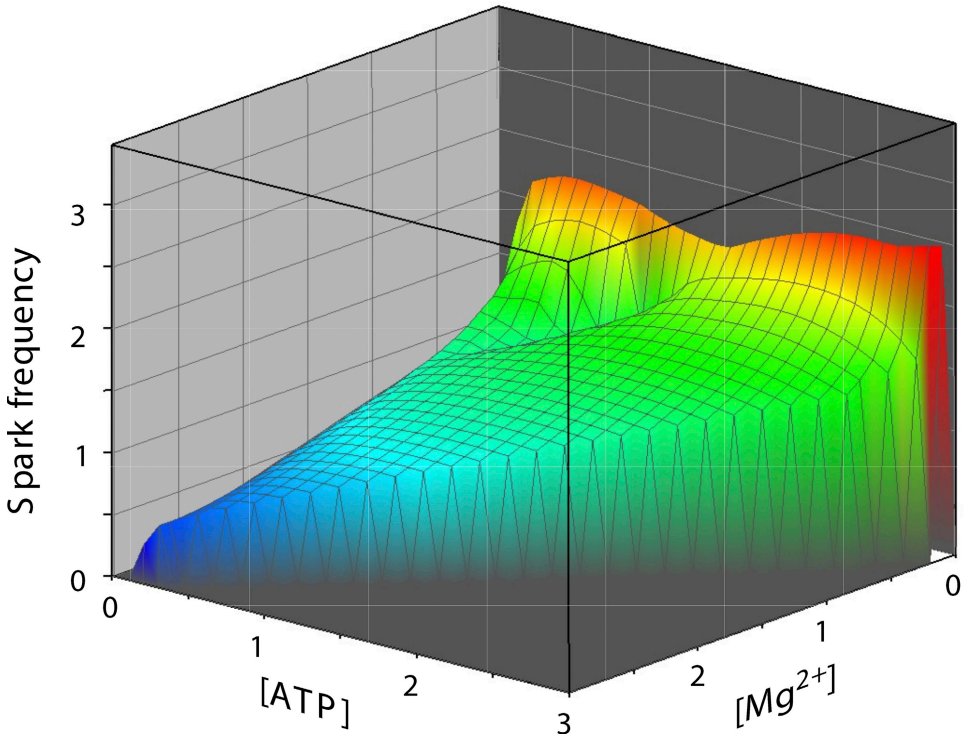

Figure 4. Ca^{2+} spark frequency is represented as a surface and is shown as a function of both $[Mg^{2+}]_{free}$ and $[ATP]_{free}$. The bivariate correlation coefficients obtained from a multivariate regression model for the Ca^{2+} spark frequency dependence on $[Mg^{2+}]_{free}$ was −0.425 (P = 0.005) and on $[ATP]_{free}$ was +0.116 (P = 0.47). For details of the multivariate analysis see Materials and methods and Table S1.

Ca^{2+} spark frequency and $[Mg^{2+}]_{free}$ with a regression coefficient of −0.45 (P = 0.005) and a weak positive association with $[ATP]_{free}$ (coefficient of +0.12; P = 0.47). When comparing $[Mg^{2+}]_{free}$ with [MgATP], the latter was found to have only a minimal inhibitory effect. For details of this analysis see Materials and methods and Table S1 (available at http://www.jgp.org/cgi/content/full/jgp.200810119/DC1). Because $[Mg^{2+}]_{free}$ and $[ATP]_{free}$ turned out to be the most important variables, we visualized the result in a two-dimensional surface plot of Ca^{2+} spark frequency as a function of both $[Mg^{2+}]_{free}$ and $[ATP]_{free}$ (Fig. 4). Overall, the surface plot also clearly reveals that $[Mg^{2+}]_{free}$ had a much stronger effect on the spark frequency than changes of $[ATP]_{free}$. For example, at the high Ca^{2+} spark frequency observed in low $[Mg^{2+}]_{free}$, reducing the ATP concentration did not lower the frequency by much. However, high free $[Mg^{2+}]_{free}$ was able to reduce the Ca^{2+} spark frequency drastically, even in the presence of a stimulatory concentration of $[ATP]_{free}$.

Free $[Mg^{2+}]$ and Spatiotemporal Parameters of the Ca^{2+} Sparks

In addition to the spark frequency we analyzed the Ca^{2+} spark amplitude, the full-width at half magnitude and the full duration at half magnitude (Fig. 6). These spatiotemporal parameters were also slightly affected, particularly in 0 and 3 mM $[Mg^{2+}]_{free}$. Lowering the Mg^{2+} level led to a reduction of the spark amplitude almost to the limit of detection. In contrast, elevated Mg^{2+} levels initially resulted in a reduction of the amplitude, which later recovered almost to control. The reduced Ca^{2+} spark amplitude reflects RYR inhibition by Mg^{2+}, but also correlates with the SR Ca^{2+} load (see Fig. 5 C).

DISCUSSION

Many ion channels and transporters are modulated by or require Mg^{2+} and ATP. Alterations of their respective concentrations, as they are known to occur, for example, during ischemia, are expected to affect the functioning of a multitude of proteins. As far as the SR and Ca^{2+} cycling are concerned, the RYRs and the SERCA appear to be particularly relevant. RYRs are known to be activated by ATP and inhibited by Mg^{2+} (Lamb, 2000; Meissner, 2004). The SERCA ultimately requires ATP to refill the SR, and the maximal Ca^{2+} gradient across the SR membrane depends on the ADP/ATP ratio (Shannon et al., 2002). Furthermore, the SERCA requires the presence of Mg^{2+} because it has a regulatory Mg^{2+} binding site (MacLennan, 1970). Thus, even on the level of SR function, changes of $[Mg^{2+}]$ and/or [ATP] may result in complex modifications of SR Ca^{2+} uptake and release.

Analysis of Ca^{2+} sparks allows observation of the Ca^{2+} release mechanism in a reasonably well-preserved structural and molecular environment in situ. As in studies with skeletal muscle fibers (Lacampagne et al., 1998; Shtifman et al., 2002; Zhou et al., 2004), we performed the experiments by using saponin-permeabilized cells under close to physiological conditions. Previous studies with RYRs reconstituted into lipid bilayers or with SR vesicles have shown that the open probability of the RYRs

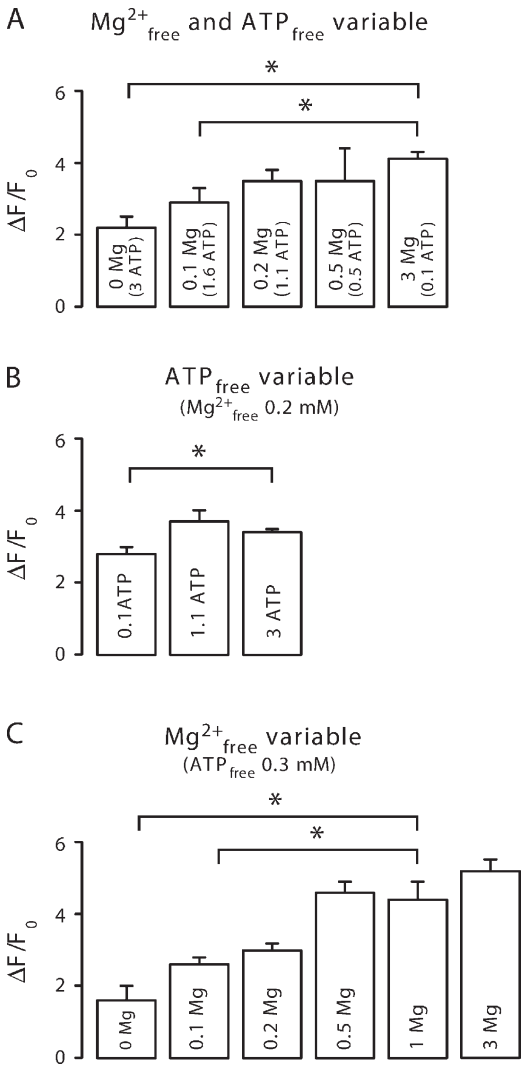

Figure 5. Dependence of SR Ca^{2+} content on the concentration of $[Mg^{2+}]_{free}$ and $[ATP]_{free}$. SR Ca^{2+} loading was estimated by application of 20 mM caffeine at the end of the experiments (after 6–8 min) and recording of the resulting fluorescence transient. (A) SR Ca^{2+} content at constant total ATP ($[Mg^{2+}]_{free}$ and $[ATP]_{free}$ varied simultaneously). (B) SR Ca^{2+} content at constant $[Mg^{2+}]_{free}$ (0.2 mM) but variable $[ATP]_{free}$. (D) SR Ca^{2+} content at constant $[ATP]_{free}$ (0.3 mM) but variable $[Mg^{2+}]_{free}$.

depends on the cytosolic concentration of free Mg^{2+} (Meissner and Henderson, 1987; Laver and Lamb, 1998; Lamb, 2000; Meissner, 2002; Laver et al., 2004; Dias et al., 2006). Besides a direct inhibition of the RYR2, Mg^{2+} can also influence its sensitivity to other modulators, particularly to caffeine, ATP, or calmodulin (Chugun et al., 2007). It was also found that the activity of SERCA depends on the level of Mg^{2+} and, ultimately, on [MgATP] (MacLennan, 1970; Smith et al., 2001). The SERCA activity will indirectly affect the Ca^{2+} sparks via SR luminal Ca^{2+} concentration, which within a cell changes according to the SR Ca^{2+} leak/uptake balance (Shannon et al., 2002). Collectively, this indicates that the effects of Mg^{2+} in cells could be quite complicated.

It should be noted that Ca^{2+} spark recordings also have some limitations. Particularly, at low $[Mg^{2+}]_{free}$ (and thus low Ca^{2+} spark amplitude), the Ca^{2+} spark frequency could be underestimated because of two reasons: (1) because the lowering of $[Mg^{2+}]_{free}$ has a tendency to initiate "macrosparks" or miniwaves (at constant $[Ca^{2+}]$), which are difficult to resolve as individual sparks; and (2) because the threshold for spark detection allows us to detect only events larger than a certain amplitude (in our case it was adjusted to 0.4 F/F_0) (Cheng et al., 1999). This may also lead to a slight underestimation of the spark frequency, especially when the average amplitude of the sparks becomes small.

Free $[Mg^{2+}]$ and Local Ca^{2+} Release Signals

Here, we assessed by which mechanism(s) changes in $[Mg^{2+}]_{free}$ modify Ca^{2+} sparks in cardiac myocytes. The experiments revealed that rapid adjustments of $[Mg^{2+}]_{free}$ result in a biphasic change of the spark frequency, suggesting indeed a complex situation. The initial transient rise (or fall) in Ca^{2+} spark frequency occurred when the level of SR Ca^{2+} loading was still close to control conditions. However, the initial change in Ca^{2+} spark frequency disturbed the uptake/leak balance of the SR, and, after some delay, the system approached a new steady-state, in which the uptake of Ca^{2+} into SR again matched the leak of Ca^{2+} through RYRs. Indeed, application of 20 mM caffeine during the new steady-state revealed that the $[Mg^{2+}]$ had a marked influence on SR Ca^{2+} content. For example, elevated $[Mg^{2+}]$ induced an accumulation of Ca^{2+} inside the SR, presumably resulting from the inhibition of the RYRs and the reduction of the Ca^{2+} leak. The opposite behavior was observed at low $[Mg^{2+}]_{free}$, where the Ca^{2+} spark activity and thus the SR Ca^{2+} leak were very pronounced. These adjustments of the luminal SR Ca^{2+} concentration also explain the observed trend of the spark frequency toward a new steady-state level after a transient increase (or decrease). In terms of Ca^{2+} spark frequency, the system approached a new equilibrium quite rapidly (with a τ_{decay} of <1 min). A similar autoregulatory tendency of SR Ca^{2+} release, albeit for signals triggered by L-type Ca^{2+} currents, has also been noted in intact cells (Eisner et al., 1998; Terentyev et al., 2002). Also, one would expect that in the steady-state Ca^{2+} sparks should disappear completely in zero MgATP because under these conditions the SERCA would stop working. Most likely, the duration of our experiments was sufficiently short to prevent total depletion of the SR Ca^{2+}. Thus, Ca^{2+} sparks were still detectable at the end of our recordings. In addition, there might be some residual Mg^{2+} within the permeabilized cells that is not yet completely washed out.

Because the free concentrations of Mg^{2+}, ATP, and MgATP are mutually dependent, all three concentrations changed during the first series of experiments, where the total $[ATP]_{total}$ remained constant. Therefore, we

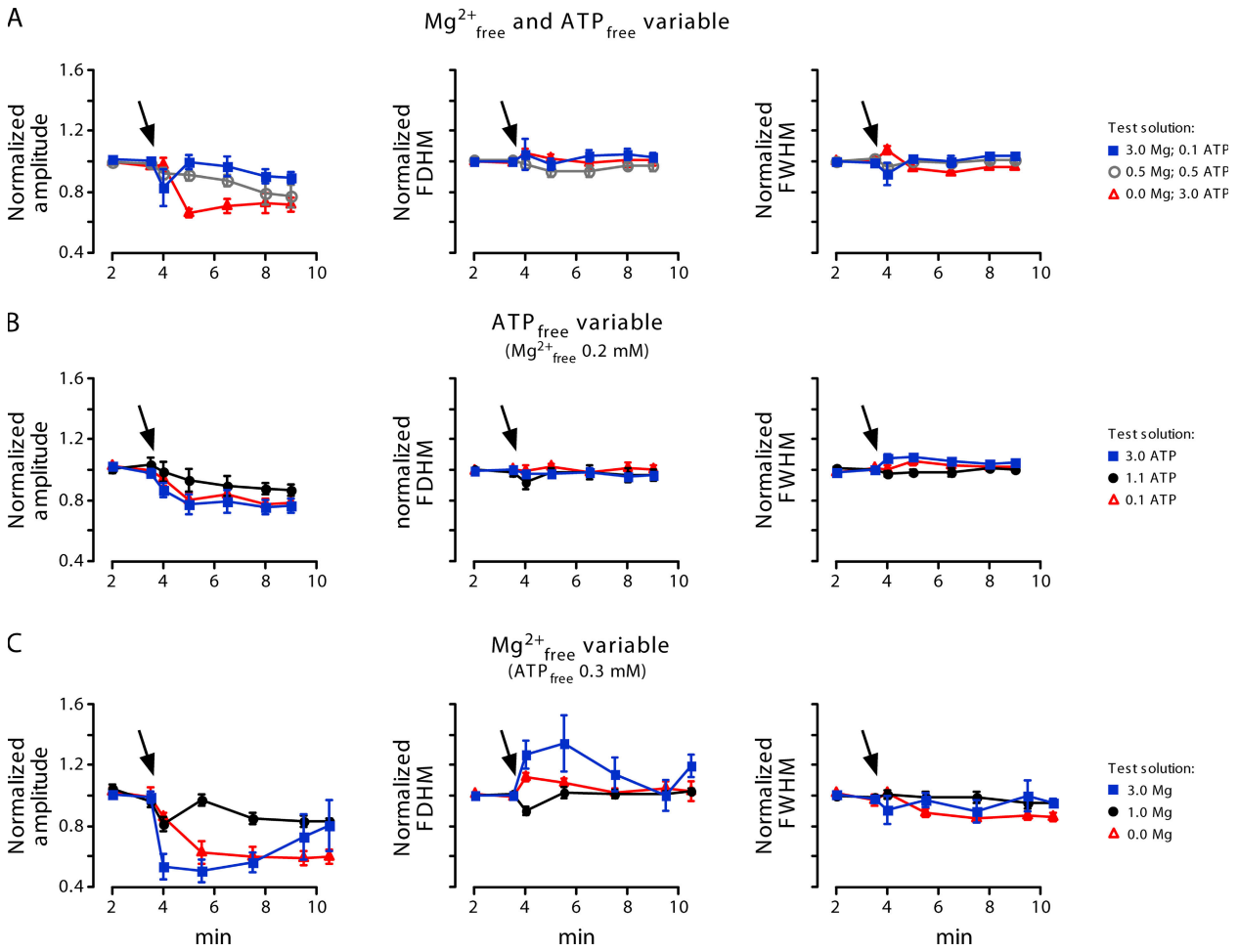

Figure 6. Summary of spatiotemporal Ca^{2+} spark parameters. Normalized amplitude, full duration at half magnitude (FDHM), and full-width at half magnitude (FWHM) are plotted versus time. Initially, all cells were in control solution, which was exchanged for test solution at the arrow. For composition of the test solution see symbol legend on the right. (A) $[Mg^{2+}]_{free}$ was varied at constant ATP_{total} (3 mM). (B) $[ATP]_{free}$ was varied at constant $[Mg^{2+}]_{free}$ (0.2 mM). (C) $[Mg^{2+}]_{free}$ was varied at constant $[ATP]_{free}$ (0.3 mM).

decided to perform additional experiments with solutions designed to keep one of these variables constant (see Table I). Using this approach we found that changes in [MgATP], as well as total $[ATP]_{total}$, did not correlate with the Ca^{2+} spark frequencies in a causal manner. Previously, ATP binding has been shown to have only a mild stimulatory effect on the cardiac RYR (Lamb, 2000), consistent with our observations. Interestingly, lowering $[ATP]_{free}$ to 0.1 mM led to a decrease in SR loading. Because this maneuver did not acutely elevate the Ca^{2+} spark frequency, the reduction in SR loading most likely did not result from enhanced RYR activation, but rather from changes of SERCA activity. ATP, as well as Mg^{2+}, also modulates SERCA2a activity. SERCA2a has a high-affinity ATP binding site (K_d ~1 μM), which is the substrate site, and a second lower-affinity site (K_d ~200 μM), which serves a regulatory role (Bers, 2001). Thus, lowering [ATP] could also decrease the transport of Ca^{2+} into the SR and induce a change in the fine balance between Ca^{2+} leak and uptake.

This result is somewhat different from the observations made by Yang and Steele (2001) in rat ventricular cardiomyocytes. In their study, the increase of the spark frequency when lowering $[ATP]_{free}$ was more pronounced and SR loading was higher at lower $[ATP]_{free}$. However, they used a higher concentration of Mg^{2+} (1 mM instead of 0.2 mM), and in most cases lower concentrations of $[ATP]_{free}$, which may explain this difference. Similarly, a much lower $[ATP]_{free}$ and higher Ca^{2+} (230 nM) may explain why ATP removal was found to inhibit the RYRs in a study on Ca^{2+} waves (Smith and O'Neill, 2001). From our Fig. 3 A it seems that under extreme conditions with a simultaneous decrease in $[ATP]_{free}$ (to 0.11 mM) and increase in $[Mg^{2+}]_{free}$ (to 3 mM), the Ca^{2+} spark frequency cannot recover to the control level. Keeping the level of $[ATP]_{free}$ constant (0.3 mM) did not change the situation (Fig. 3 C). Thus, increasing the SR Ca^{2+} content was not sufficient to overcome the suppressed RYR activity under these conditions. The low SR Ca^{2+} content despite suppressed RYR activity most likely

underlies the low activity state of CICR found under these conditions.

Possible Mechanisms for Ca^{2+} Spark Inhibition by Mg^{2+}

The initial transient changes of the Ca^{2+} spark frequency most likely resulted from a direct interaction of Mg^{2+} with the RYRs because secondary adjustments of SR Ca^{2+} content had not yet developed. In previous studies on the single-channel level in lipid bilayers, it has been noted that the RYR2 has at least two binding sites for modulation by Mg^{2+}, and both sites can also bind Ca^{2+} (Laver et al., 1997a; Lamb, 2000). Ca^{2+} activates the RYR by binding at the activating site (or A-site) with a K_i of ~1 µM. The affinity of the A-site for Mg^{2+} is ~40-fold lower, and Mg^{2+} binding at the A-site prevents activation of the channel by Ca^{2+} (Laver and Honen, 2008). The inhibitory I-site of the RYR2 has a very low Ca^{2+} affinity ($K_i > 1$ mM), but a similar affinity for Mg^{2+}. Binding of either ion inactivates the channel. These findings suggest that, at a low Ca^{2+} concentration, Mg^{2+} acts mostly at the activation site, particularly when $[Mg^{2+}]_{free}$ is <1 mM. However, increasing $[Mg^{2+}]_{free}$ will inhibit RYRs further via the inhibitory site.

Fitting the Mg^{2+} dependence of the Ca^{2+} spark frequencies observed here by a Hill equation for inhibition (Laver et al., 2004):

$$SpF_0 = SpF_{max}/(1+([Mg^{2+}]_i/K_i)^n,$$

where SpF is spark frequency, yielded a K_i = 0.35 mM, n = 0.86, when both $[Mg^{2+}]_i$ and [ATP] were changing. For the data where only $[Mg^{2+}]_{free}$ was changing and $[ATP]_{free}$ remained constant at 0.3 mM, the K_i was 0.1 mM and n = 0.66. Thus, the observed K_i for Ca^{2+} spark generation (~0.1 mM) is in the range of the Mg^{2+} affinity of the A-site on the RYR2 (see above). This suggests that the main mechanism of Ca^{2+} spark suppression by Mg^{2+} is by binding to the A-site of the RYRs, which is in contrast to skeletal muscle (Laver et al., 1997a). Mg^{2+} binding to the A-site, which competes with binding of activating Ca^{2+} to the same site, is most likely also responsible for the reduced Ca^{2+} spark amplitude observed in elevated $[Mg^{2+}]_{free}$.

Interestingly, when we kept the $[ATP]_{free}$ constant at 0.3 mM, the steady-state Ca^{2+} spark frequency was quite different from the situation with a constant total ATP. This observation is consistent with a regulatory effect of ATP on the modulation by $[Mg^{2+}]$, which has been shown for skeletal muscle (Jona et al., 2001), and which may be present in cardiac muscle too.

Implications of the Results Obtained

Under physiological conditions, cellular-free $[ATP]_i$ and $[Mg^{2+}]_i$ levels are tightly regulated and very stable. However, both $[Mg^{2+}]_i$ and $[ATP]_i$ are altered during ischemia (Murphy et al., 1989; Kléber, 1990). While the concentration of free (and total) $[ATP]_i$ declines, the concentration of $[Mg^{2+}]_i$ becomes elevated. Besides the disruption of other ATP-dependent processes, these pathological disturbances of the intracellular milieu and the release of free Mg^{2+} will affect the Ca^{2+} homeostasis and several ion channels (Bers, 2001). In particular, the elevation of $[Mg^{2+}]_i$ will inhibit the RYRs, subsequently limiting the Ca^{2+} release from the SR. This suppression of the CICR is thought to be beneficial for the survival of the ischemic cardiomyocytes because it will dramatically reduce the energy demand of the affected cells. During ischemia, other factors, such as the acidic pH, will contribute to RYR2 inhibition and CICR shutdown, leading to a highly Ca^{2+}-loaded SR (Overend et al., 2001). Therefore, for a complete appreciation of disease-related alterations of Ca^{2+} spark and Ca^{2+} signaling, a better understanding of isolated processes is required, such as the mechanism of RYR inhibition by Mg^{2+} as characterized here. To this end, several computer models incorporating the interactions of Mg^{2+} with Ca^{2+} signaling in cardiac cells have been developed (Laver et al., 1997a; Zahradnikova et al., 2003; Michailova et al., 2004; Valent et al., 2007) and our present data should enable further progress in these efforts.

The authors thank Dr. Peter Jueni for advice on the biostatistics and Daniel Luethi for technical assistance.

This work was supported by the Swiss National Science Foundation (grant 31-109693 to E. Niggli), the Swiss Cardiovascular Research and Training Network (SCRTN), and the Swiss Foundation for Research on Muscle Diseases.

Lawrence G. Palmer served as editor.

Submitted: 11 September 2008
Accepted: 30 October 2008

REFERENCES

Ashley, R.H., and A.J. Williams. 1990. Divalent cation activation and inhibition of single calcium release channels from sheep cardiac sarcoplasmic reticulum. *J. Gen. Physiol.* 95:981–1005.

Berridge, M.J. 2006. Calcium microdomains: organization and function. *Cell Calcium.* 40:405–412.

Bers, D.M. 2001. Excitation-Contraction Coupling and Cardiac Contractile Force. Kluwer, Dordrecht, Netherlands. 427 pp.

Blatter, L.A., and J.A.S. McGuigan. 1986. Free intracellular magnesium concentration in ferret ventricular muscle measured with ion selective micro-electrodes. *Q. J. Exp. Physiol.* 71:467–473.

Cheng, H., W.J. Lederer, and M.B. Cannell. 1993. Calcium sparks: elementary events underlying excitation-contraction coupling in heart muscle. *Science.* 262:740–744.

Cheng, H., L.S. Song, N. Shirokova, A. Gonzalez, E.G. Lakatta, E. Rios, and M.D. Stern. 1999. Amplitude distribution of calcium sparks in confocal images: theory and studies with an automatic detection method. *Biophys. J.* 76:606–617.

Chugun, A., O. Sato, H. Takeshima, and Y. Ogawa. 2007. Mg^{2+} activates the ryanodine receptor type 2 (RyR2) at intermediate Ca^{2+} concentrations. *Am. J. Physiol. Cell Physiol.* 292:C535–C544.

Copello, J.A., S. Barg, A. Sonnleitner, M. Porta, P. Diaz-Sylvester, M. Fill, H. Schindler, and S. Fleischer. 2002. Differential activation by Ca^{2+}, ATP and caffeine of cardiac and skeletal muscle ryanodine receptors after block by Mg^{2+}. *J. Membr. Biol.* 187:51–64.

DelPrincipe, F., M. Egger, and E. Niggli. 1999. Calcium signalling in cardiac muscle: refractoriness revealed by coherent activation. *Nat. Cell Biol.* 1:323–329.

Dias, J.M., C. Szegedi, I. Jona, and P.D. Vogel. 2006. Insights into the regulation of the ryanodine receptor: differential effects of Mg^{2+} and Ca^{2+} on ATP binding. *Biochemistry.* 45:9408–9415.

Eisner, D.A., A.W. Trafford, M.E. Diaz, C.L. Overend, and S.C. O'Neill. 1998. The control of Ca release from the cardiac sarcoplasmic reticulum: regulation versus autoregulation. *Cardiovasc. Res.* 38:589–604.

Fabiato, A., and F. Fabiato. 1975. Effects of magnesium on contractile activation of skinned cardiac cells. *J. Physiol.* 249:497–517.

Gyorke, S., and D. Terentyev. 2008. Modulation of ryanodine receptor by luminal calcium and accessory proteins in health and cardiac disease. *Cardiovasc. Res.* 77:245–255.

Hess, P., P. Metzger, and R. Weingart. 1982. Free magnesium in sheep, ferret and frog striated muscle at rest measured with ion-selective micro-electrodes. *J. Physiol.* 333:173–188.

Jona, I., C. Szegedi, S. Sarkozi, P. Szentesi, L. Csernoch, and L. Kovacs. 2001. Altered inhibition of the rat skeletal ryanodine receptor/calcium release channel by magnesium in the presence of ATP. *Pflugers Arch.* 441:729–738.

Keller, M., J.P. Kao, M. Egger, and E. Niggli. 2007. Calcium waves driven by "sensitization" wave-fronts. *Cardiovasc. Res.* 74:39–45.

Kermode, H., A.J. Williams, and R. Sitsapesan. 1998. The interactions of ATP, ADP, and inorganic phosphate with the sheep cardiac ryanodine receptor. *Biophys. J.* 74:1296–1304.

Kléber, A.G. 1990. Consequences of acute ischemia for the electrical and mechanical function of the ventricular myocardium. A brief review. *Experientia.* 46:1162–1167.

Lacampagne, A., M.G. Klein, and M.F. Schneider. 1998. Modulation of the frequency of spontaneous sarcoplasmic reticulum Ca^{2+} release events (Ca^{2+} sparks) by myoplasmic [Mg^{2+}] in frog skeletal muscle. *J. Gen. Physiol.* 111:207–224.

Lamb, G.D. 2000. Excitation-contraction coupling in skeletal muscle: comparisons with cardiac muscle. *Clin. Exp. Pharmacol. Physiol.* 27:216–224.

Laver, D.R. 2005. Coupled calcium release channels and their regulation by luminal and cytosolic ions. *Eur. Biophys. J.* 34:359–368.

Laver, D.R., and B.N. Honen. 2008. Luminal Mg^{2+}, a key factor controlling RYR2-mediated Ca^{2+} release: cytoplasmic and luminal regulation modeled in a tetrameric channel. *J. Gen. Physiol.* 132:429–446.

Laver, D.R., and G.D. Lamb. 1998. Inactivation of Ca^{2+} release channels (ryanodine receptors RyR1 and RyR2) with rapid steps in [Ca^{2+}] and voltage. *Biophys. J.* 74:2352–2364.

Laver, D.R., T.M. Baynes, and A.F. Dulhunty. 1997a. Magnesium inhibition of ryanodine-receptor calcium channels: evidence for two independent mechanisms. *J. Membr. Biol.* 156:213–229.

Laver, D.R., V.J. Owen, P.R. Junankar, N.L. Taske, A.F. Dulhunty, and G.D. Lamb. 1997b. Reduced inhibitory effect of Mg^{2+} on ryanodine receptor-Ca^{2+} release channels in malignant hyperthermia. *Biophys. J.* 73:1913–1924.

Laver, D.R., E.R. O'Neill, and G.D. Lamb. 2004. Luminal Ca^{2+}-regulated Mg^{2+} inhibition of skeletal RyRs reconstituted as isolated channels or coupled clusters. *J. Gen. Physiol.* 124:741–758.

Lukyanenko, V., S. Viatchenko-Karpinski, A. Smirnov, T.F. Wiesner, and S. Gyorke. 2001. Dynamic regulation of sarcoplasmic reticulum Ca^{2+} content and release by luminal Ca^{2+}-sensitive leak in rat ventricular myocytes. *Biophys. J.* 81:785–798.

MacLennan, D.H. 1970. Purification and properties of an adenosine triphosphatase from sarcoplasmic reticulum. *J. Biol. Chem.* 245:4508–4518.

Meissner, G. 2002. Regulation of mammalian ryanodine receptors. *Front. Biosci.* 7:2072–2080.

Meissner, G. 2004. Molecular regulation of cardiac ryanodine receptor ion channel. *Cell Calcium.* 35:621–628.

Meissner, G., and J.S. Henderson. 1987. Rapid calcium release from cardiac sarcoplasmic reticulum vesicles is dependent on Ca^{2+} and is modulated by Mg^{2+}, adenine nucleotide, and calmodulin. *J. Biol. Chem.* 262:3065–3073.

Michailova, A.P., M.E. Belik, and A.D. McCulloch. 2004. Effects of magnesium on cardiac excitation-contraction coupling. *J. Am. Coll. Nutr.* 23:514S–517S.

Murphy, E., C. Steenbergen, L.A. Levy, B. Raju, and R.E. London. 1989. Cytosolic free magnesium levels in ischemic rat heart. *J. Biol. Chem.* 264:5622–5627.

Niggli, E. 1999. Localized intracellular calcium signaling in muscle: calcium sparks and calcium quarks. *Annu. Rev. Physiol.* 61:311–335.

Niggli, E., and N. Shirokova. 2007. A guide to sparkology: the taxonomy of elementary cellular Ca^{2+} signaling events. *Cell Calcium.* 42:379–387.

Otsu, K., H.F. Willard, V.K. Khanna, F. Zorzato, N.M. Green, and D.H. MacLennan. 1990. Molecular cloning of cDNA encoding the Ca^{2+} release channel (ryanodine receptor) of rabbit cardiac muscle sarcoplasmic reticulum. *J. Biol. Chem.* 265:13472–13483.

Overend, C.L., D.A. Eisner, and S.C. O'Neill. 2001. Altered cardiac sarcoplasmic reticulum function of intact myocytes of rat ventricle during metabolic inhibition. *Circ. Res.* 88:181–187.

Rios, E., N. Shirokova, W.G. Kirsch, G. Pizarro, M.D. Stern, H. Cheng, and A. Gonzalez. 2001. A preferred amplitude of calcium sparks in skeletal muscle. *Biophys. J.* 80:169–183.

Shannon, T.R., K.S. Ginsburg, and D.M. Bers. 2002. Quantitative assessment of the SR Ca^{2+} leak-load relationship. *Circ. Res.* 91:594–600.

Shtifman, A., C.W. Ward, T. Yamamoto, J. Wang, B. Olbinski, H.H. Valdivia, N. Ikemoto, and M.F. Schneider. 2002. Interdomain interactions within ryanodine receptors regulate Ca^{2+} spark frequency in skeletal muscle. *J. Gen. Physiol.* 119:15–32.

Smith, G.A., J.I. Vandenberg, N.S. Freestone, and H.B. Dixon. 2001. The effect of Mg^{2+} on cardiac muscle function: is CaATP the substrate for priming myofibril cross-bridge formation and Ca^{2+} reuptake by the sarcoplasmic reticulum? *Biochem. J.* 354:539–551.

Smith, G.L., and S.C. O'Neill. 2001. A comparison of the effects of ATP and tetracaine on spontaneous Ca^{2+} release from rat permeabilised cardiac myocytes. *J. Physiol.* 534:37–47.

Szentesi, P., C. Pignier, M. Egger, E.G. Kranias, and E. Niggli. 2004. Sarcoplasmic reticulum Ca^{2+} refilling controls recovery from Ca^{2+}-induced Ca^{2+} release refractoriness in heart muscle. *Circ. Res.* 95:807–813.

Terentyev, D., S. Viatchenko-Karpinski, H.H. Valdivia, A.L. Escobar, and S. Gyorke. 2002. Luminal Ca^{2+} controls termination and refractory behavior of Ca^{2+}-induced Ca^{2+} release in cardiac myocytes. *Circ. Res.* 91:414–420.

Valent, I., A. Zahradnikova, J. Pavelkova, and I. Zahradnik. 2007. Spatial and temporal Ca^{2+}, Mg^{2+}, and ATP^{2-} dynamics in cardiac dyads during calcium release. *Biochim. Biophys. Acta.* 1768:155–166.

Wang, S.Q., L.S. Song, E.G. Lakatta, and H. Cheng. 2001. Ca^{2+} signalling between single L-type Ca^{2+} channels and ryanodine receptors in heart cells. *Nature.* 410:592–596.

Williams, I.A., and D.G. Allen. 2007. Intracellular calcium handling in ventricular myocytes from mdx mice. *Am. J. Physiol. Heart Circ. Physiol.* 292:H846–H855.

Yang, Z., and D.S. Steele. 2001. Effects of cytosolic ATP on Ca^{2+} sparks and SR Ca^{2+} content in permeabilized cardiac myocytes. *Circ. Res.* 89:526–533.

Zahradnikova, A., M. Dura, I. Gyorke, A.L. Escobar, I. Zahradnik, and S. Gyorke. 2003. Regulation of dynamic behavior of cardiac ryanodine receptor by Mg^{2+} under simulated physiological conditions. *Am. J. Physiol. Cell Physiol.* 285:C1059–C1070.

Zhou, J., B.S. Launikonis, E. Rios, and G. Brum. 2004. Regulation of Ca^{2+} sparks by Ca^{2+} and Mg^{2+} in mammalian and amphibian muscle. An RyR isoform-specific role in excitation-contraction coupling? *J. Gen. Physiol.* 124:409–428.